The vertical distribution of buoyant plastics at sea: an observational study in the North Atlantic Gyre

J. Reisser[1*], B. Slat[2*], K. Noble[3], K. du Plessis[4], M. Epp[1], M. Proietti[5], J. de Sonneville[2], T. Becker[6], and C. Pattiaratchi[1]

*These authors contributed equally as co-first authors

[1] School of Civil, Environmental and Mining Engineering and UWA Oceans Institute, University of Western Australia, Australia

[2] The Ocean Cleanup Foundation, The Netherlands

[3] Roger Williams University, USA

[4] Pangaea Exploration, USA

[5] Instituto de Oceanografia, Universidade Federal do Rio Grande, Brazil

[6] Centre for Microscopy, Characterisation and Analysis, University of Western Australia, Australia

Correspondence to: J. Reisser (jureisser@gmail.com)

Abstract

Millimeter-sized plastics are numerically abundant and widespread across the world's ocean surface. These buoyant macroscopic particles can be mixed within the upper water column due to turbulent transport. Models indicate that the largest decrease in their concentration occurs within the first few meters of water, where *in situ* observations are very scarce. In order to investigate the depth profile and physical properties of buoyant plastic debris, we used a new type of multi-level trawl at 12 sites within the North Atlantic subtropical gyre to sample from the air-seawater interface to a depth of 5 m, at 0.5 m intervals. Our results show that plastic concentrations drop exponentially with water depth, and decay rates decrease with increasing Beaufort scale. Furthermore, smaller pieces presented lower rise velocities and were more susceptible to vertical transport. This resulted in higher depth decays of plastic mass concentration (milligrams m^{-3}) than numerical concentration (pieces m^{-3}). Further multi-level sampling of plastics will improve our ability to predict at-sea plastic load, size distribution, drifting pattern, and impact on marine species and habitats.

1 Introduction

Plastics pose physical and chemical threats to the oceans' ecosystem. Their widespread occurrence at the sea surface may be shifting the distribution and abundance of marine populations due to (1) enhanced ocean drift opportunities and (2) damaging effects on biota and habitats. Plastics harbour organisms - such as fouling microorganisms, invertebrates, and fish - that can widely disperse via this new type of habitat, potentially entering non-native waters (Winston et al., 1997;Barnes, 2002;Thiel and Gutow, 2005;Zettler et al., 2013;Reisser et al., 2014). Plastic objects can also entangle or be ingested/inhaled by marine animals, leading to impacts such as starvation, death, and hepatic stress (Derraik, 2002;Browne et al., 2008;Gregory, 2009;Rochman et al., 2013;Watts et al., 2014).

Most of what is known about at-sea plastic characteristics and concentrations comes from surface net sampling, where the top few centimetres of the water column is filtered to collect plastics larger than 0.2–0.4 mm (Hidalgo-Ruz et al., 2012). These sea surface samples have shown that the world's sea surface contains many millimetre-sized plastic pieces known as 'microplastics' when smaller than 5 mm in length (Arthur et al., 2009;Hidalgo-Ruz et al., 2012). This type of plastic pollution is widespread across oceans, with higher contamination levels at convergence zones such as those within subtropical gyres (Carpenter and Smith, 1972;Maximenko et al., 2012;Lebreton et al., 2012;van Sebille et al., 2012;Cózar et al., 2014;Eriksen et al., 2014). Plastic debris collected by surface nets are mostly fragments of packaging and fishing gear made of polyethylene and polypropylene (Barnes et al., 2009;Morét-Ferguson et al., 2010;Hidalgo-Ruz et al., 2012;Reisser et al., 2013). These two resins are less dense than seawater and account for approximately 62% of the plastic volume produced each year (Andrady, 2011).

Turbulence in the upper-ocean layer can vertically mix buoyant plastic particles. A model developed by Kukulka et al. 2012 predicted that the largest decrease in plastic concentration occurs over the first meters of the water column, where only a few low-resolution measurements exist (Lattin et al., 2004;Doyle et al., 2011;Kukulka et al., 2012;Isobe et al., 2014). As studying ocean turbulent transport is heavily dependent on observations (Ballent et al., 2012;D'Asaro, 2014), high-resolution multi-level plastic sampling is urgently needed to test this prediction. A better understanding of the vertical transport of buoyant plastics is fundamental for improving estimates of concentration, size distribution, and dispersal of

plastics in the world's ocean (Kukulka et al., 2012;Reisser et al., 2013;Law et al., 2014;Isobe et al., 2014).

In this context, the present study aimed at obtaining depth profiles of plastic pollution in the top layer of the oceans (0-5 m). We performed multi-level sampling with a new type of equipment to (1) quantify the exponential decay rates of plastic mass and numerical concentration with depth, and (2) demonstrate how these vary with sea state. We also provide the first experimental measurements of the rise velocity of plastic pieces, evaluating its relation to the type and size of pieces.

2 Materials and Methods

2.1 At-sea sampling

We conducted 12 multi-level net tows that sampled the upper 5 meters of the North Atlantic accumulation zone (Law et al., 2010;Maximenko et al., 2012;Lebreton et al., 2012) during day hours, from 19 to 22 May 2014, aboard the sailing vessel Sea Dragon (Figure 1). We used a new collection device capable of sampling surface waters from the air-seawater interface to a depth of 5 m, at 0.5 m intervals. This equipment is composed of eleven frames with 0.5 m height x 0.3 m width fitted with 2.1 m-long 150 μm mesh polyester nets. These nets were stacked vertically and secured within an external frame that was dragged in the water from eight towing points, ensuring its stability and perpendicular position in relation to the sea surface, with the top net completely above mean water line (see Figure 1). Tow durations ranged from 55 to 60 minutes and were all undertaken while the vessel was travelling at a speed of 1–1.9 knots. The captain, who has 20 years sailing experience, estimated wind speeds and sea state of each sampling period: Beaufort scale 1 (N = 3 net tows), 3 (N = 4 net tows), and 4 (N = 5 net tows) (Reisser et al., 2015). After each tow, we transferred the collected contents to a 150 μm sieve and stored them in aluminium bags that were kept frozen during transportation.

2.2 Estimating depth profiles of plastic contamination

We calculated plastic numerical and mass concentrations by dividing the number of plastic pieces and total plastic mass by the volume of filtered seawater of each net sample (pieces m^{-3}

and milligrams m^{-3}). Filtered volume was estimated using frame dimensions and readings from a mechanical flowmeter (32 cm per rotation).

Samples were washed into a clear plastic container filled with filtered seawater, and floating macroscopic plastics were organised into gridded petri dishes for counting and characterisation. The searches for plastic pieces were of at least one hour per sample, with the aid of thumb forceps, dissecting needles, magnifying glasses, and LED torches. The latter was particularly important for detecting thin transparent plastic fragments, which had low detection probability when not reflecting light. Two thin filaments resembling textile fibres were discarded due to potential air contamination as noted in (Foekema et al., 2013). Once all plastics were counted and characterised, they were washed with deionised water, transferred to aluminium dishes, dried at 60° C, and weighed.

To quantify the variation of plastic concentration with depth and assess the effect of changing sea state on these vertical profiles, we first divided plastic concentration of samples by their correspondent surface concentration value. We then took the average of these normalised concentrations between adjacent nets to estimate normalised plastic concentration values at depths of: 0 m (top 2 nets), 1 m (3rd and 4th nets), 2 m (5th and 6th nets), 3 m (7th and 8th nets), 4 m (9th and 10th), and 4.75 m (11th net). Finally, numerical and mass concentration values from tows collected under same Beaufort scale were grouped and fitted to exponential decay models of the form $N = e^{-\lambda z}$, where N = normalised plastic concentration, z = depth, and λ = decay rate.

We also predicted normalised plastic concentration depth profiles using the model described in Kukulka et al. (2012): $N = e^{zw_b A_0^{-1}}$, where z = depth, w_b = plastic rise velocity, and $A_0 = 1.5 u_{*w} k H_s$ with u_{*w} = frictional velocity of water, k = 0.4 (von Karman constant), and H_s = significant wave height. We considered w_b = 0.0053 m s^{-1} (plastics' median rise velocity, as estimated in this study), H_s = 0.1 m, 0.6 m, or 1m (typical wave heights experienced at Beaufort scales 1, 3, and 4, respectively), and used the wind ranges of Beaufort 1, 3, and 4 (1-3 knots, 7-10 knots, and 11-16 knots, respectively) to estimate their respective u_{*w} values through the approximation proposed by (Pugh, 1987): $u_{*w} = 0.00012 W_{10}$, where W_{10} = ten-metre wind speed in m/s. Thus, the considered numerical ranges of frictional velocity of water (u_{*w}) were: 0.0006-0.0019 m s^{-1} for Beaufort scale 1, 0.0043 – 0.0062 m s^{-1} for Beaufort scale 3, and 0.0068-0.0099 m s^{-1} for Beaufort scale 4.

2.3 Characterising plastic length, type, resin, and rise velocity

We measured the length of all plastic pieces using a transparent ruler (0.5 mm resolution), and classified them into the following types: hard plastic - fragments of rigid plastic; sheet - fragments of thin plastic, with some degree of flexibility; line - fragments of fishing lines or nets; foam - expanded polystyrene fragments; and pellet - raw material used to produce plastic items (Fotopoulou and Karapanagioti, 2012). We also identified the resin composition of 60 pieces using Raman spectroscopy (WITec alpha 300RA+), and measured the rise velocity of 0-3 plastics from each sample collected.

Our method of rise velocity measurement is an adaptation of an experiment to examine the fall velocity of various types of sediment particles in different fluids (Allen, 1985). Firstly, we made two marks 12.5 cm from the ends of a 1 m long clear plastic tube (diameter = 40 mm). Secondly, we filled the tube with filtered seawater, capped both its ends with rubber stops, and locked it in place with a clamp. One of the tube ends was then opened, a plastic piece placed inside, the tube closed again (with no trapped air), and quickly turned upside down and locked in place with a clamp, using a spirit level to adjust its vertical position. Finally, we recorded the time taken for the plastic piece to rise from one mark to the other (distance = 75 cm) using a stopwatch. This was measured 4 times per plastic piece, and the average was used as the estimation of its rise velocity (w_b). Rise velocities of different plastic types were separately plotted against plastic lengths (l), and linear regressions of the form $w_b = al + b$ were applied to assess the effect of plastics' characteristics on its rise velocity. We also plotted the rise velocities of plastic pieces collected at different depths to visualise depth patterns.

Finally, we calculated the fractions of plastics of different size classes (0.5-1 mm, 1.5-2 mm, 2.5-3 mm, 3.5-4 mm, 4.5-5 mm, > 5.5 mm) that were located at the sea surface (depth < 0.5 m) and in deeper layers (depth > 0.5 m) during sampling at Beaufort scales 1, 3, and 4. We calculated these fractions using all plastics collected, as well as separated by plastic type.

3 Results

3.1 Depth profiles of mass and numerical concentrations

Plastic numerical and mass concentrations both decreased abruptly from their peak values at the sea surface, where median values were equal to 1.69 pieces m^{-3} and 1.60 mg m^{-3} (Figure 2). Concentration differences between surface and deeper layers were higher in terms of mass than number of particles. For instance, median mass and numerical concentrations at 0.5-1 m were respectively 13.3 and 6.5 times lower than their median plastic peaks at 0-0.5 m.

Exponential models fitted well with both numerical and mass concentrations (R^2 = 0.99–0.84), with depth decay rates (λ) consistently higher for mass than numerical concentration. Furthermore, both numerical and mass concentration decay rates were inversely proportional to Beaufort state (Figure 3). Depth decay rate of numerical concentration went from 3.0 at Beaufort 1 (95% confidence interval - 95%CI = 2.56-3.45), to 1.7 at Beaufort 3 (95%CI = 1.51-1.88), and 0.8 at Beaufort 4 (95%CI = 0.62-0.98). Decay rate of mass concentration went from 3.8 at Beaufort 1 (95%CI = 3.23-4.33), to 2.4 at Beaufort 3 (95%CI = 1.63-3.14), and 1.7 at Beaufort 4 (95%CI = 1.50-1.94).

These exponential fits had relatively similar depth decay rates to those predicted by Kukulka's model for Beaufort 3 (λ = 2.36–3.37) and 4 (λ = 0.88–1.28). However, for Beaufort 1 the statistical fit showed much smaller λ (2.56-4.33) than those predicted by Kukulka's model (λ = 141.73–47.2492).

3.2 Lengths, types, resins and rise velocities of plastics

We counted and classified 12,751 macroscopic plastic pieces with lengths varying from 0.5 to 207 mm (median = 1.5 mm; Figure 4). They were mostly fragments of polyethylene (84.7%), followed by polypropylene (15.3%) items. Hard plastics (46.6%) and sheets (45.4%) were predominant, with lower presence of plastic lines (7.9%), pellets (0.05%) and foams (0.008%).

Plastic rise velocity ranged from 0.001 to 0.0438 m/s (Figure 5a). It was directly proportional to plastic length, with the slope of this linear relationship differing among types of plastic (Figure 5b). While both hard plastics and sheets had a slope equal to 0.002 (95% CI = 0.0017-0.0026 and 0.0012-0.0023, respectively), plastic lines had a flatter slope of 0.00007 (95% CI = 0.00002-0.00013), since their rise velocity increased only slightly towards longer pieces.

Rise velocities differed among sampled depths, with particles at the surface (0-0.5 m) having a wider range of values and a higher median value than pieces at greater depths (Figure 5c).

The vertical mixing process was size-selective, and affected the size distribution of plastics located at the sea surface (Figure 6), with the proportion of plastics at depths over 0.5 m generally increasing towards smaller plastic lengths (Figure 7). For hard plastics and sheets, this trend was observed at all Beaufort scales sampled. Plastic lines however, only displayed this trend at Beaufort 1, with different size classes showing similar and relatively high underwater proportions at Beaufort 3 and 4.

Datasets produced and analysed in this study are available at Figshare (Reisser et al., 2015).

4 Discussion

This study describes high-resolution depth profiles of plastic concentrations, which were shown to decrease exponentially with depth, with decay rates decreasing towards stronger winds. It also provides the first measurements of the rise velocity of ocean plastics, which varies with particle size and type. Furthermore, it shows that depth profiles of plastic mass are associated with higher decay rates than depth profiles of plastic numbers. This can be explained by our observation of smaller/lighter plastic pieces generally associated with lower rising velocities, being therefore more susceptible to vertical transport.

Predictions of plastic vertical mixing are commonly used to correct numerical concentrations obtained by surface net sampling (Kukulka et al., 2012;Reisser et al., 2013;Cózar et al., 2014;Law et al., 2014). As determined in our study, the model described in Kukulka et al. (2012) performed relatively well in estimating the total number of plastic pieces at the wind-mixed surface layer. The major difference between this model and our observations occurred at the calmest sea state condition (Beaufort scale 1): while the model predicted that all plastics would be at the surface, we still observed some particles submerged at depths greater than 0.5 m below the water surface. This could have been a consequence of the presence of other types of vertical flow at our sampled sites (e.g. downwelling) or the occurrence of plastics rising from deeper waters due to previous wind-driven mixing events.

Our results indicate that plastic numerical concentration decays at a lower rate than plastic mass concentration, as smaller plastics are more susceptible to vertical transport. The uncertainties related to how plastic numerical concentration translates into plastic mass

concentration have already led to differences between plastic load estimates arising from different studies. For instance, Cózar et al. (2014) used a correlation based on simultaneous surface tow measurements of total mass and abundance of plastic to convert depth-integrated numerical concentrations into mass concentrations. These authors estimated that the total plastic load in the world's sea surface layer is between 7,000 and 35,000 tons. On the other hand, Law et al. (2014) multiplied depth-integrated numerical concentrations by the average plastic particle mass (1.36×10^{-5} kg), and estimated that the microplastic load at the North Pacific accumulation zone alone is of at least 21,290 tons. Such differences evidence the importance of better predicting the vertical transport of ocean plastics to develop standard plastic load estimation methods. More sampling is required to better quantify both profiles of plastic mass and numerical concentration over a broader range of sea states, and translate these observations into prediction models. Such models may need to be three-dimensional, and account not only for wind mixing effects, but also ocean plastic properties (e.g. particle size) and other types of vertical transport processes (e.g. Langmuir circulation).

As shown here, and in two modelling studies (Ballent et al., 2012;Isobe et al., 2014), vertical mixing affects the size distribution of plastics floating at the surface. We observed that the proportion of plastics mixed into deeper waters increases towards smaller sizes even under low wind speed (1 knot) conditions (see Figure 7). This observation has implications for studies assessing size distribution of plastics using surface sampling devices. Cózar et al. (2014) and Eriksen et al. (2014) quantified the size distribution of ocean plastics from worldwide sampling locations and concluded that there are major losses of small plastics from the sea surface. Here we show that at least a fraction of this 'missing' plastic could be just under the sampled surface layer (0-0.5 m). For instance, 20% of 0.5-1 mm, 13% of 1.5-2 mm, and 8% of 2.5-3 mm long plastics were between 0.5 and 5 m deep during our Beaufort scale 1 net tows. More at-sea and experimental work is required to further quantify this effect and estimate depth-integrated size distribution of buoyant plastics drifting at sea.

Predicting the vertical mixing of buoyant plastics is also important as it affects the horizontal drifting patterns and ecological impacts of plastic pollution. For instance, larger pieces of plastic coming from land-based sources may stay trapped near the shore until further fragmentation, due to a combination of their high buoyancy and the effect of Stokes drift produced by waves parallel to coastlines (Isobe et al., 2014). Furthermore, the vertical distribution of plastics will influence the likelihood of animals inhabiting different depths to

encounter, and potentially interact, with plastic. For instance, sea birds, turtles, and mammals, which breathe air and use the sea surface for daily activities, present high rates of plastic ingestion and entanglement (Derraik, 2002;Tourinho et al., 2010). These high interaction rates could be partly explained by the relatively high concentrations of plastic debris at the sea surface, as shown in this study.

Our findings show that vertical mixing affects the number, mass, and size distribution of buoyant plastics captured by surface nets, a standard equipment for at-sea plastic pollution sampling (Hidalgo-Ruz et al., 2012). Subsurface samples are still scarce and the processes influencing distribution of plastics throughout the ocean's water column are poorly understood. Further multi-level sampling across a broader range of sea states is necessary for better quantifying the vertical mixing of buoyant plastics. This will improve predictions of ocean plastic concentration levels (Kukulka et al., 2012), size distributions (Cózar et al., 2014;Eriksen et al., 2014), drifting patterns (Isobe et al., 2014), and interactions with neustonic and pelagic species of the world's oceans.

Acknowledgements

We thank The Ocean Cleanup and The University of Western Australia for funding, Pangaea Exploration for sea time, and the staff and crew of our expedition: Eric Loss, Shanley McEntee, Winston Ricardo, Bart Sturm, Beatrice Clyde-Smith, Kasey Erin, Mario Merkus, Max Muller, and Jennifer Gelin. The authors also acknowledge The Ocean Cleanup volunteers who helped design, build, and test the multi-level trawl (see http://www.theoceancleanup.com for details). J Reisser received IPRS, UWA Completion, and CSIRO Postgraduate scholarships.

References

Allen, J.: Sink or swim?, Physical Sedimentology, Springer, 1985.

Andrady, A. L.: Microplastics in the marine environment, Marine Pollution Bulletin, 62, 1596-1605, 2011.

Arthur, C., Baker, J., and Bamford, H.: Proceedings of the International Research Workshop on the Occurrence, Effects, and Fate of Microplastic Marine Debris, September 9-11, 2008, 2009.

Ballent, A., Purser, A., Mendes, P. d. J., Pando, S., and Thomsen, L.: Physical transport properties of marine microplastic pollution, Biogeosciences Discussions, 9, 18755, 2012.

Barnes, D. K.: Biodiversity: invasions by marine life on plastic debris, Nature, 416, 808-809, 2002.

Barnes, D. K. A., Galgani, F., Thompson, R. C., and Barlaz, M.: Accumulation and fragmentation of plastic debris in global environments, Philosophical Transactions of the Royal Society B: Biological Sciences, 364, 1985-1998, 2009.

Browne, M. A., Dissanayake, A., Galloway, T. S., Lowe, D. M., and Thompson, R. C.: Ingested microscopic plastic translocates to the circulatory system of the mussel, *Mytilus edulis* (L.), Environmental Science & Technology, 42, 5026-5031, 2008.

Carpenter, E. J., and Smith, K.: Plastics on the Sargasso Sea Surface, Science, 175, 1240-1241, 1972.

Cózar, A., Echevarría, F., González-Gordillo, J. I., Irigoien, X., Úbeda, B., Hernández-León, S., Palma, Á. T., Navarro, S., García-de-Lomas, J., and Ruiz, A.: Plastic debris in the open ocean, Proceedings of the National Academy of Sciences, 111, 10239-10244, 2014.

D'Asaro, E. A.: Turbulence in the upper-ocean mixed layer, Annual Review of Marine Science, 6, 101-115, 2014.

Derraik, J. G.: The pollution of the marine environment by plastic debris: a review, Marine Pollution Bulletin, 44, 842-852, 2002.

Doyle, M. J., Watson, W., Bowlin, N. M., and Sheavly, S. B.: Plastic particles in coastal pelagic ecosystems of the Northeast Pacific ocean, Marine Environmental Research, 71, 41-52, 2011.

Eriksen, M., Lebreton, L. C. M., Carson, H. S., Thiel, M., Moore, C. J., Borerro, J. C., Galgani, F., Ryan, P. G., and Reisser, J.: Plastic Pollution in the World's Oceans: More than 5 Trillion Plastic Pieces Weighing over 250,000 Tons Afloat at Sea, PLOS ONE, 9, e111913, 2014.

Foekema, E. M., De Gruijter, C., Mergia, M. T., van Franeker, J. A., Murk, A. J., and Koelmans, A. A.: Plastic in North sea fish, Environmental Science & Technology, 47, 8818-8824, 2013.

Fotopoulou, K. N., and Karapanagioti, H. K.: Surface properties of beached plastic pellets, Marine Environmental Research, 2012.

Gregory, M. R.: Environmental implications of plastic debris in marine settings—entanglement, ingestion, smothering, hangers-on, hitch-hiking and alien invasions,

Philosophical Transactions of the Royal Society B: Biological Sciences, 364, 2013-2025, 2009.

Hidalgo-Ruz, V., Gutow, L., Thompson, R. C., and Thiel, M.: Microplastics in the marine environment: a review of the methods used for identification and quantification, Environmental Science & Technology, 46, 3060-3075, 2012.

Isobe, A., Kubo, K., Tamura, Y., Nakashima, E., and Fujii, N.: Selective transport of microplastics and mesoplastics by drifting in coastal waters, Marine Pollution Bulletin, 2014.

Kukulka, T., Proskurowski, G., Morét‐Ferguson, S., Meyer, D., and Law, K.: The effect of wind mixing on the vertical distribution of buoyant plastic debris, Geophysical Research Letters, 39, 1-6, 2012.

Lattin, G. L., Moore, C. J., Zellers, A. F., Moore, S. L., and Weisberg, S. B.: A comparison of neustonic plastic and zooplankton at different depths near the southern California shore, Marine Pollution Bulletin, 49, 291-294, 2004.

Law, K. L., Morét-Ferguson, S., Maximenko, N. A., Proskurowski, G., Peacock, E. E., Hafner, J., and Reddy, C. M.: Plastic accumulation in the North Atlantic subtropical gyre, Science, 329, 1185-1188, 2010.

Law, K. L., Moret-Ferguson, S., Goodwin, D. S., Zettler, E. R., DeForce, E., Kukulka, T., and Proskurowski, G.: Distribution of surface plastic debris in the eastern Pacific Ocean from an 11-year dataset, Environmental Science & Technology, 2014.

Lebreton, L.-M., Greer, S., and Borrero, J.: Numerical modelling of floating debris in the world's oceans, Marine Pollution Bulletin, 64, 653-661, 2012.

Maximenko, N., Hafner, J., and Niiler, P.: Pathways of marine debris derived from trajectories of Lagrangian drifters, Marine Pollution Bulletin, 65, 51-62, 2012.

Morét-Ferguson, S., Law, K. L., Proskurowski, G., Murphy, E. K., Peacock, E. E., and Reddy, C. M.: The size, mass, and composition of plastic debris in the western North Atlantic Ocean, Marine Pollution Bulletin, 60, 1873-1878, 2010.

Pugh, D. T.: Tides, surges and mean sea-level: a handbook for engineers and scientists., John Wiley & Sonschichester, Chichester, 1987.

Reisser, J., Shaw, J., Wilcox, C., Hardesty, B. D., Proietti, M., Thums, M., and Pattiaratchi, C.: Marine plastic pollution in waters around Australia: characteristics, concentrations, and pathways, PLOS ONE, 8(11), e80466, 2013.

Reisser, J., Shaw, J., Hallegraeff, G., Proietti, M., Barnes, D. K., Thums, M., Wilcox, C., Hardesty, B. D., and Pattiaratchi, C.: Millimeter-sized marine plastics: a new pelagic habitat for microorganisms and invertebrates, PLOS ONE, 9, e100289, 2014.

Reisser, J., Slat, B., Noble, K., du Plessis, K., Epp, M., Proietti, M., de Sonneville, J., Becker, T., and Pattiaratchi, C.: Data from 'The vertical ditribution of buoyant plastics at sea: an observational study in the North Atlantic Gyre', Figshare, 2015.

Rochman, C. M., Hoh, E., Kurobe, T., and Teh, S.: Ingested plastic transfers hazardous chemicals to fish and induces hepatic stress, Nature, 3: 3263, 10.1038/srep03263, 2013.

Thiel, M., and Gutow, L.: The ecology of rafting in the marine environment. II. The rafting organisms and community, Oceanography and Marine Biology: An Annual Review, 43, 279-418, 2005.

Tourinho, P. S., Ivar do Sul, J. A., and Fillmann, G.: Is marine debris ingestion still a problem for the coastal marine biota of southern Brazil?, Marine Pollution Bulletin, 60, 396-401, 2010.

van Sebille, E., England, M. H., and Froyland, G.: Origin, dynamics and evolution of ocean garbage patches from observed surface drifters, Environmental Research Letters, 7, 044040, 2012.

Watts, A. J., Lewis, C., Goodhead, R. M., Beckett, S. J., Moger, J., Tyler, C. R., and Galloway, T. S.: Uptake and retention of microplastics by the shore crab Carcinus maenas, Environmental Science & Technology, 48, 8823-8830, 2014.

Winston, J. E., Gregory, M. R., and Stevens, L. M.: Encrusters, epibionts, and other biota associated with pelagic plastics: a review of biogeographical, environmental, and conservation issues, in: Marine Debris, Springer, 81-97, 1997.

Zettler, E. R., Mincer, T. J., and Amaral-Zettler, L. A.: Life in the 'Plastisphere': Microbial communities on plastic marine debris, Environmental Science & Technology, 47, 7137-7146, 2013.

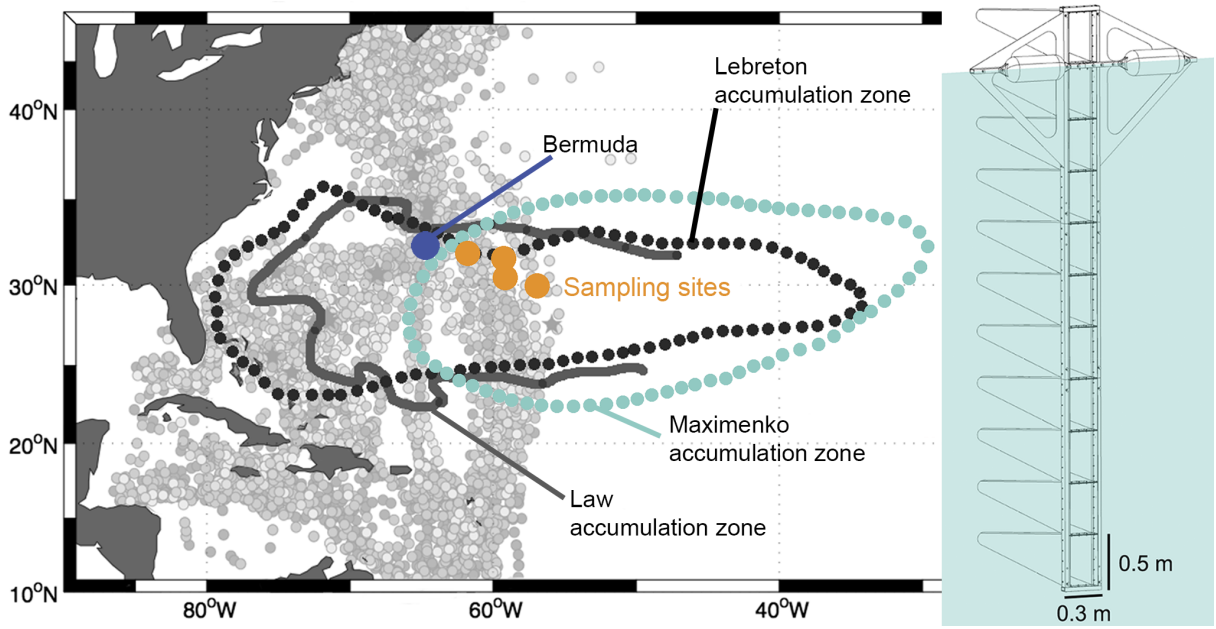

Figure 1. North Atlantic map indicating locations sampled during this study (orange dots) using the multi-level net displayed in the right panel. The four orange dots include all 12 multi-level net tows conducted in the study, which could not be shown separately due to scale. The map also shows the expedition departure and arrival location (Bermuda), as well as plastic accumulation zones predicted by ocean modelling (dotted lines) (Lebreton et al., 2012;Maximenko et al., 2012), and a surface net tow dataset (solid gray line; grey dots show locations of net tows) (Law et al., 2010).

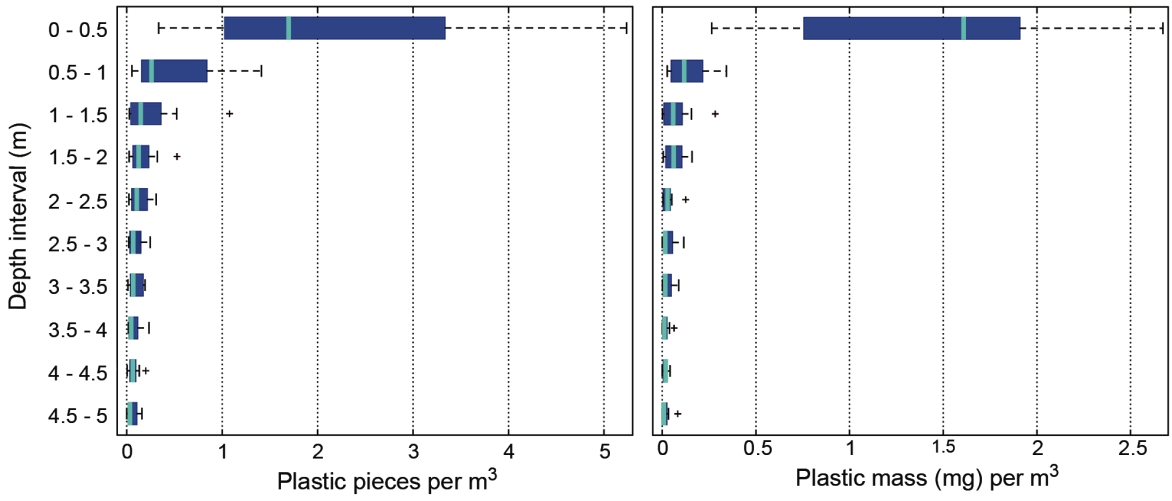

Figure 2. Boxplots of plastic numerical (left) and mass (right) concentrations at different depth intervals (N = 12 multi-level net tows). The central line is the median value, edges of the box are the 25th and 75th percentiles, whiskers extend to extreme data points not considered outliers, and outliers are plotted individually as crosses.

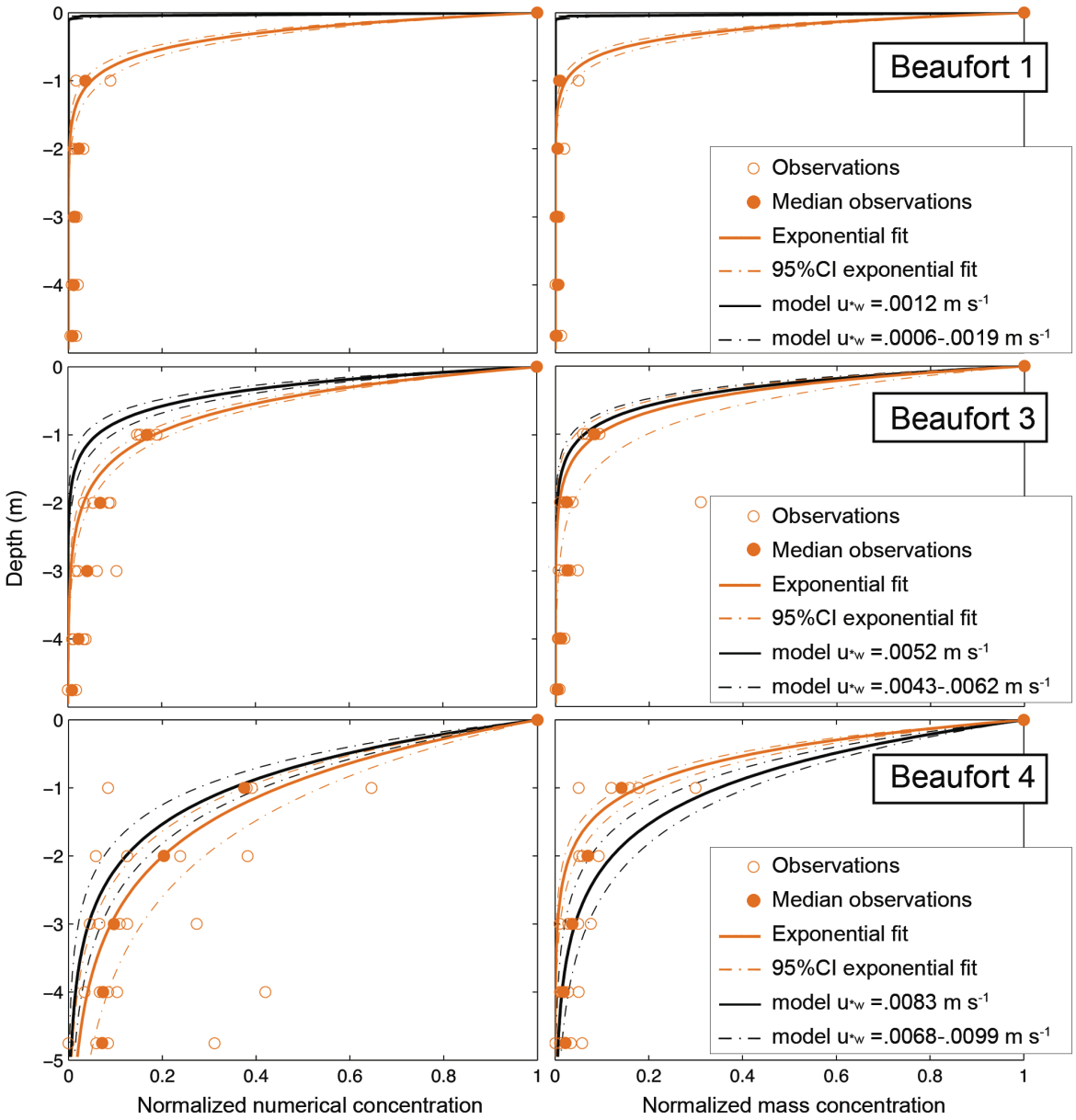

Figure 3. Depth profiles of normalized plastic numerical and mass concentrations under different Beaufort scales: 1 (N = 3 net tows; 3283 plastic pieces), 3 (N = 4 net tows; 4049 plastic pieces), and 4 (N = 5 net tows; 5419 plastic pieces). Black lines show model predictions (Kukulka et al., 2012) using median plastic rise velocity (0.0053 m/s), and the typical range of frictional velocity of water (u_{*w}) at each of the sea states sampled.

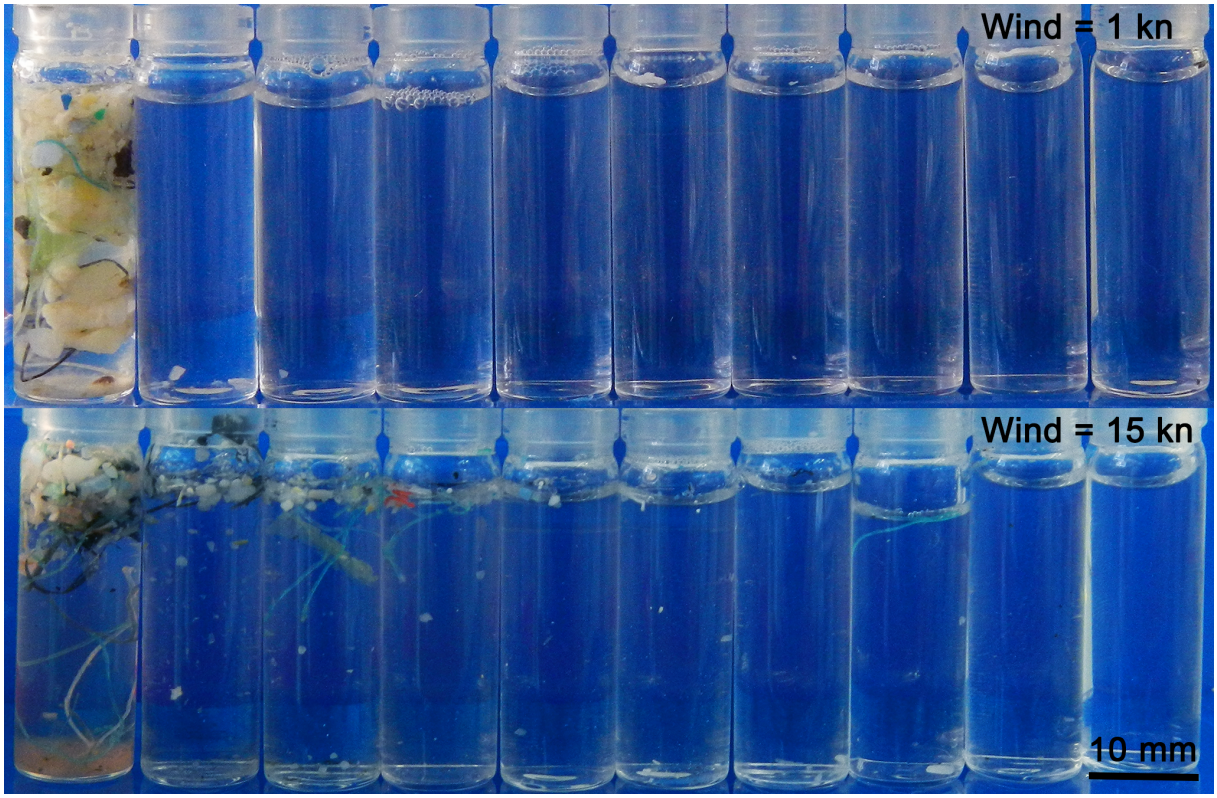

Figure 4. Glass jars with filtered water and plastic samples collected under wind speeds of 1 knot (Beaufort scale 1, top image) and 15 knots (Beaufort scale 4, bottom image). From left to right: 0 – 0.5 m, 0.5 – 1 m, 1 – 1.5 m, 1.5 – 2 m, 2 – 2.5 m, 2.5 – 3 m, 3 – 3.5 m, 3.5 – 4 m, 4 – 4.5 m, and 4.5 – 5 m depth intervals.

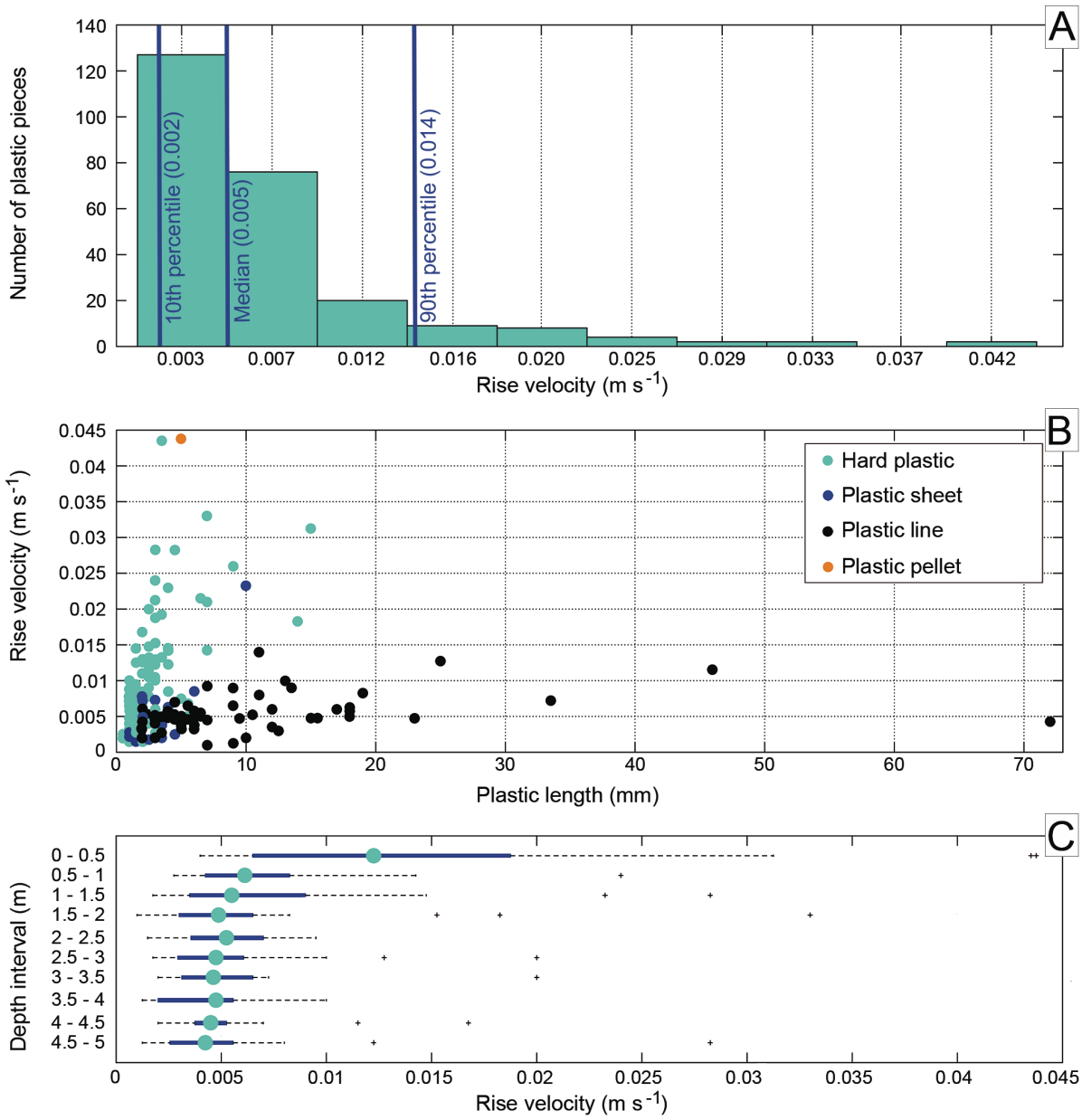

Figure 5. Histogram of rise velocity of plastics (A), plots of plastic sizes versus rise velocities of different types of plastic (B), and boxplot of rise velocity for plastics collected at different depth intervals (C). In C, the central dot is the median value, edges of the box are the 25th and 75th percentiles, whiskers extend to extreme data points not considered outliers, and outliers are plotted individually as crosses.

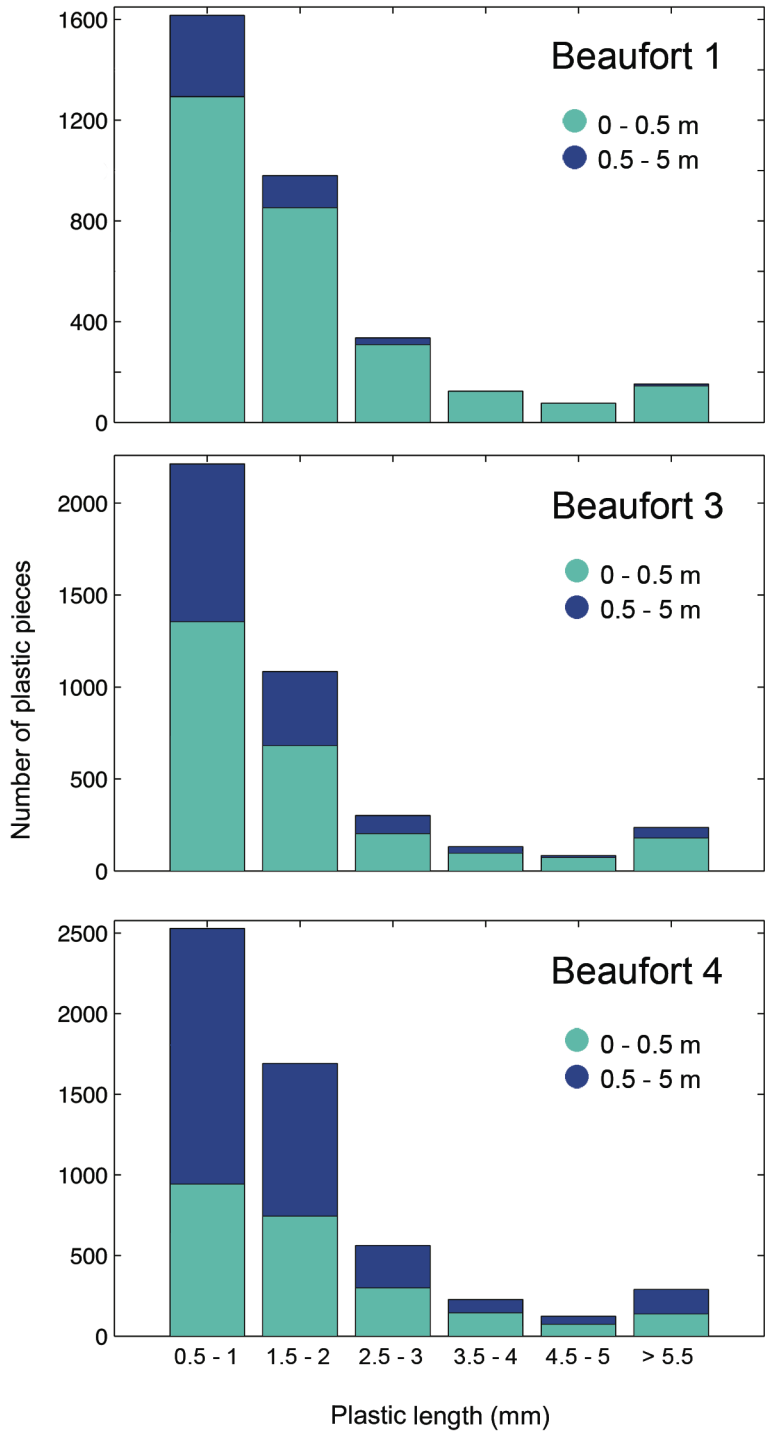

Figure 6. Size histograms of plastics collected at depths 0-0.5 m and 0.5-5 m during Beaufort scale 1 (top panel), 3 (middle panel), and 4 (bottom panel).

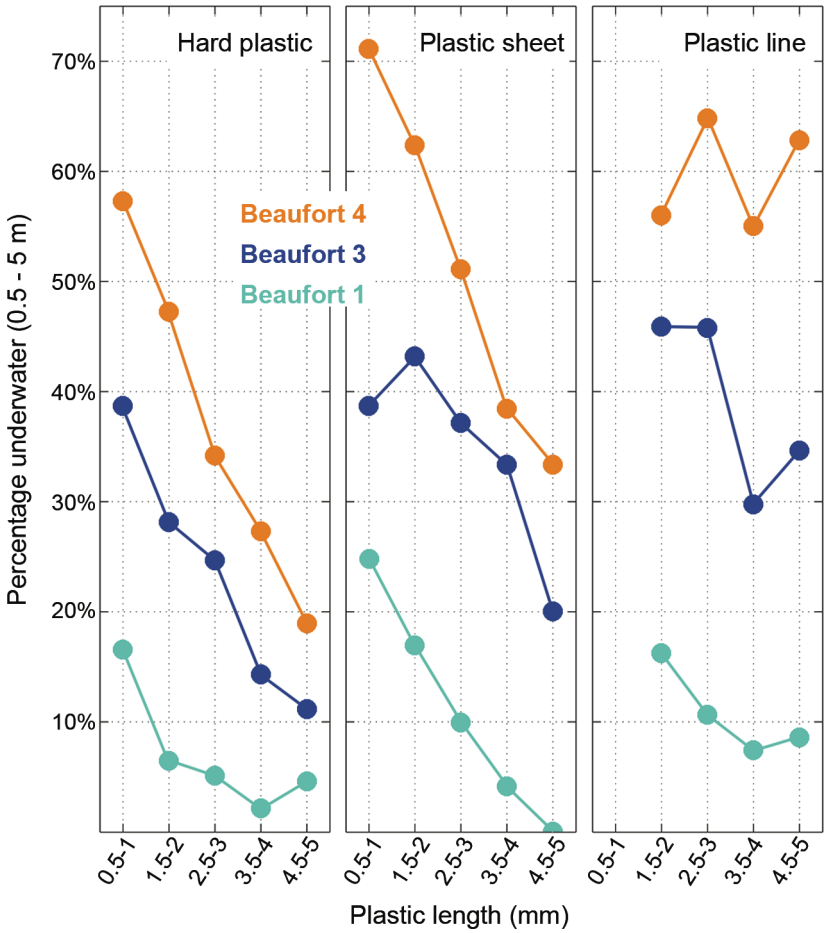

Figure 7: Percentage of plastic pieces of different types and size classes located at depths greater than 0.5 m during sampling at Beaufort scale 1, 3, and 4.